NANO LETTERS

Letter

pubs.acs.org/NanoLett

Tunable Charge Transport in Single-Molecule Junctions via Electrolytic Gating

Brian Capozzi,[†] Qishui Chen,[‡] Pierre Darancet,[§] Michele Kotiuga,[§] Marisa Buzzeo,[∥] Jeffrey B. Neaton,[§] Colin Nuckolls,[‡] and Latha Venkataraman*[,†]

[†]Department of Applied Physics and Mathematics and [‡]Department of Chemistry, Columbia University, New York, New York, United States

[§]Molecular Foundry, Materials Sciences Division, Lawrence Berkeley National Laboratory, and Department of Physics, University of California, Berkeley, California, United States

[∥]Department of Chemistry, Barnard College, New York, New York, United States

Supporting Information

ABSTRACT: We modulate the conductance of electrochemically inactive molecules in single-molecule junctions using an electrolytic gate to controllably tune the energy level alignment of the system. Molecular junctions that conduct through their highest occupied molecular orbital show a decrease in conductance when applying a positive electrochemical potential, and those that conduct though their lowest unoccupied molecular orbital show the opposite trend. We fit the experimentally measured conductance data as a function of gate voltage with a Lorentzian function and find the fitting parameters to be in quantitative agreement with self-energy corrected density functional theory calculations of transmission probability across single-molecule junctions. This work shows that electrochemical gating can directly modulate the alignment of the conducting orbital relative to the metal Fermi energy, thereby changing the junction transport properties.

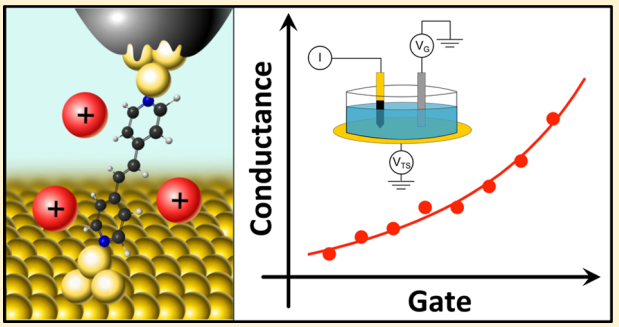

KEYWORDS: *Electrochemical gating, single-molecule junctions, density functional theory, electronic transport, break-junctions*

There has been significant interest in the field of single-molecule electronics both from the standpoint of learning fundamental physics and for potentially leading to a further miniaturization of electronic components.[1] While molecular junctions, individual molecules attached to two metal electrodes, are most commonly studied in a source-drain device geometry,[2−5] a molecular junction with a gate electrode in a transistor configuration gives an additional knob with which to tune the transport characteristics. Creating such molecular transistors in a three-terminal geometry is not trivial, as it is very challenging to fabricate an effective gate electrode in close enough proximity to the conducting molecular junction. Recent experiments that have relied on electromigration fabrication techniques have demonstrated some gating in such three terminal devices.[6−9] An attractive alternative to back-gating is electrolyte gating, where large gate efficiencies can be achieved. Recently, both organic and semiconductor field effect transistors and nanotube or graphene devices[10,11] made using ionic liquids, electrolyte solutions, or polymer electrolytes as gate dielectrics have received significant attention due to their ability to generate large interfacial capacitances on the nanoscale, thereby enhancing gate efficiencies.[12−17] These large capacitances result from the formation of electric double layers at solution/material interfaces, whose width is on the order of the electrolyte size (approximately a few nanometers) allowing large electric fields to develop across this layer.

For nanoscale molecular junctions in particular, electrolytic gating should enable much more efficient electrostatic coupling since the electric double layer will exist regardless of the position of the gate electrode in solution. While several groups have applied an electrochemical gating technique to study transport in electrochemically active molecules that change their charge state,[18−22] the continuous modulation of the conductance of a non-redox active molecule has not been demonstrated. Here, we present the electrolytic gating of several molecules that reproducibly and consistently change their conductance upon application of gate biases despite being electrochemically inactive in the potential ranges studied. In particular, we show that the conductance of a molecular junction can be tuned with an electrochemical gate potential analogous to what can be achieved using an electrostatic gate. We find that molecules that conduct through the lowest unoccupied molecular orbital (LUMO, n-type) show an increase (decrease) in conductance with positive (negative)

Received: December 2, 2013
Revised: January 24, 2014

dx.doi.org/10.1021/nl404459q | *Nano Lett.* XXXX, XXX, XXX−XXX

gate potentials, while molecules that conduct through the highest occupied molecular orbital (HOMO, p-type) show the opposite trend. Furthermore, modeling the transmission functions of these molecules with a single Lorentzian lineshape, we are able to extract orbital coupling and molecular resonance position that agree well with self-energy corrected density functional theory (DFT) calculations. This quantitative agreement between experiment and theory demonstrates that in gating the molecular junctions we are indeed probing transport as a function of energy along the transmission curve.

In order to study the conductance ($G = I/V$) of single-molecule junctions, we use the scanning tunneling microscope-based break junction (STM-BJ) technique. In this technique, a mechanically cut Au tip is repeatedly driven into and out of contact with an Au-on-mica substrate in a solution of a target molecule using a custom STM setup that has been described in detail previously.[3] Electrolytic gating is implemented using an Au substrate and an Apiezon wax-coated Au tip[23] that serve as the source and drain electrodes and a Pt wire electrode that serves as the gate electrode as illustrated in Figure 1a.[10] The Au

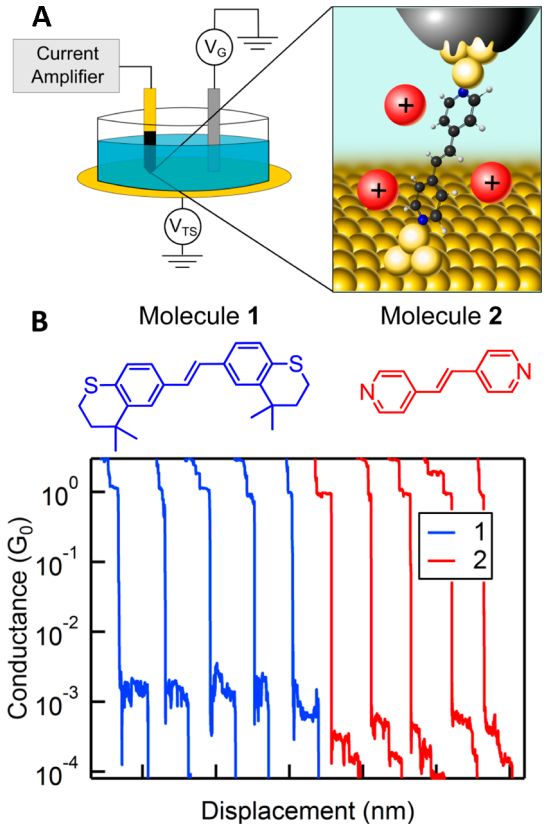

Figure 1. (A) Schematic of experimental setup and cartoon of a single molecule being gated in a junction. (B) Molecular structures of **1** and **2** along with several sample conductance traces for each molecule measured with a tip−sample voltage of 25 mV and at zero gate potential.

electrodes can also be considered the working electrode in our system while the Pt wire can be considered the counter electrode. The exposed areas of the insulated tips are ~1 μm. Conductance measurements are then carried out in a fluid cell with ~1 mM solutions of the target molecule in propylene carbonate with tetrabutylammonium perchlorate (0.1 M) serving as the supporting electrolyte. For each molecule, 2000−3000 conductance traces are collected at multiple gate electrode potentials (that is, our gate potential is applied to the Pt electrode) with the source-drain bias fixed at 25 mV.

We carry out break junction measurements on 1,2-bis(4,4-dimethylthiochroman-6-yl)ethylene (**1**), which is synthesized following procedures detailed previously,[24] and 1,2-bis(4-pyridyl)ethylene (**2**), which is obtained from Sigma-Aldrich and used without further purification (Figure 1b). Molecule **1** conducts through the HOMO while molecule **2** conductance through the LUMO as determined by calculations detailed below in the manuscript. Conductance traces display plateaus near integer multiples of the quantum of conductance (G_0, $2e^2/h$) with an additional plateau in a molecule-specific range below G_0; these additional features indicate the formation of metal−molecule−metal junctions (Figure 1c). In order to analyze the data, each set of traces at a given gate potential is compiled into a linearly binned conductance histogram (without data selection) where frequently occurring conductance values now appear as peaks in the histogram. The most probable junction conductance is then obtained by fitting a Lorentzian to the conductance peak.[3] We note here that the conductance histograms for all molecules studied here are very similar to those carried out without a gate electrode or the supporting electrolyte.[24,25]

For **1**, the HOMO conducting molecule, the peak present in the conductance histogram clearly shifts to lower values as the applied gate potential is increased from −1.1 to 2.5 V (Figure 2a). Figure 2b displays the conductance histogram peak values against the applied gate potential, where the conductance changes by roughly a factor of 2 over the entire gate potential range. The inset of Figure 2a shows full conductance histograms at two gate potentials, showing clear peaks at integer multiples of G_0 indicating that Au point contacts form regardless of gate potential. We note that the height of the molecular conductance peak decreases with application of increasingly negative gate potentials due to a decrease in length of the plateaus seen in individual traces as the gate potential is made to be more negative (see two-dimensional histograms shown in the Supporting Information). For molecule **1**, we find that the applied potential can vary from −1.1 to +2.5 V; we do not see molecular conductance plateaus outside this window. At gate potentials more negative than −1.1 V, we attribute the lack of plateaus to a weakening of the Au−S donor−acceptor bond that anchors the molecule to the gold leads. Because molecule **1** binds through HOMO, as the gate potential is made more negative, the HOMO gets closer to the Fermi level, E_F, as will be discussed in detail below. This increases charge transfer between the molecule and the electrode and weakens the Au−S donor−acceptor bond. At applied gate potentials more positive than +2.5 V, we no longer observe junction formation, possibly due to the Au getting oxidized and preventing junctions from forming.

The LUMO conducting molecule, **2**, shows two peaks in its conductance histograms, corresponding to two distinct binding configurations:[25] a higher conducting, tilted geometry (high-G), and a lower conducting, vertical geometry (low-G). Both peaks shift toward higher conductance values as the applied gate potential is increased from −1 V to +2.5 V (Figure 2c), and for both geometries, the conductance peak shifts by approximately a factor of 3 over the entire gate voltage range (Figure 2d). The inset of Figure 2c shows conductance histograms at two gate potentials, displaying the continued formation of gold point contacts. In contrast to the

dx.doi.org/10.1021/nl404459q | Nano Lett. XXXX, XXX, XXX−XXX

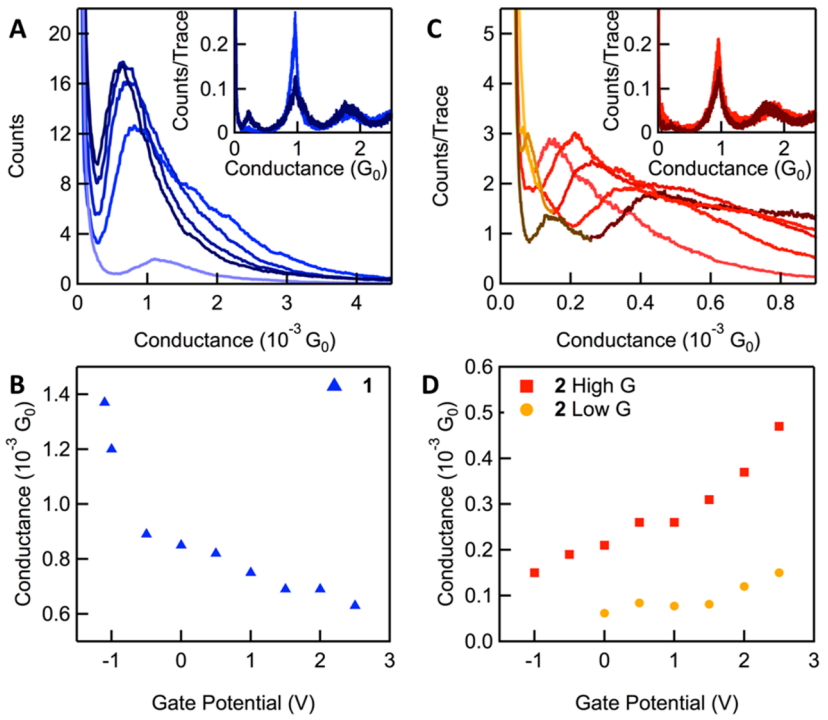

Figure 2. (A,C) Sample conductance histograms at gate potentials V_G = 2.5, 2, 1, 0, and −1 V darkest to lightest for molecule **1** and **2** respectively. Note: for molecule **2** red shades indicate the high-G conductance feature while orange shades indicate the low-G conductance feature. Inset: Conductance histograms at two gate potentials showing the continued formation of Au point contacts (peak at $1G_0$). (B,D) Peak conductance values versus applied gate potential for **1** and **2**, respectively.

conductance peak of molecule **1**, the peak heights for both high- and low-G features of molecule **2** do not change dramatically over the range of gate potentials. This difference can be rationalized by considering the location of the HOMO orbital for **2** relative to E_F. Because the HOMO orbital for **2** is far from E_F,[25] small changes in its alignment due to the applied gate do not result in a weakening of the Au−N donor−acceptor bond. As the gate voltage is made more negative than −1 V however, the low-G peak drops below the instrument noise and the high-G peak becomes a shoulder against the noise background. At positive gate voltages beyond 2.5 V, we stop observing junctions as in the measurements with **1**. Again, neither molecule undergoes a redox event in this gate bias window (see CV curves in Supporting Information), yet we clearly see that the gate bias modulates the measured conductance. This same procedure was repeated for 4,4′-bipyridine (see Supporting Information).

To understand these directional conductance shifts, we consider the effect of the gate potential on the alignment of frontier orbital resonance energy relative to the tip/substrate Fermi energy. Applying a positive potential to the gate electrode causes a buildup of anions (−ve) about the gate electrode while inducing a buildup of cations (+ve) about the Au electrodes and the molecular junction (a negative gate potential results in a build up of anions about the Au electrodes and the molecular junction). The double layer formed at the Au electrodes and about the molecular junction alters the energy difference between the electrode Fermi energy and the relevant junction frontier resonance energy (i.e., the molecular HOMO or LUMO which can be thought of as the molecules "valence band" and "conduction band," respectively). Analogous to a field effect transistor, the build-up of charge about the molecule and electrodes acts to electrostatically shift the molecular orbitals relative to the vacuum level and to E_F of the electrodes. Placing more positive (negative) charge in the vicinity of the molecule causes a downshift (upshift) in the molecular orbitals, bringing LUMO (HOMO) closer to E_F while pushing HOMO (LUMO) further away. Concomitantly, a layer of positive charge on the electrodes raises the energy required to remove an electron, thereby increasing the work function of the electrode. The arrangement of electrolyte both near the molecule and on the electrodes cooperatively changes the local potential at the molecule, altering level alignment and conductance. Along similar lines, a change in electrode work function has been previously shown to explain the variation in conductance observed for molecules in different solvents.[26]

On the basis of this discussion, we can now use the gate-dependent conductance data to determine the alignment of the conducting orbital to E_F. We first relate the applied gate potential (applied between the Pt counter electrode and the instrument ground) to the potential drop at the working electrode (tip and substrate), as we also have in these measurements a significant potential drop across the Pt electrode/solution interface. We relate the applied potential to the potential drop at the working electrode by comparing linear sweep voltammograms of a solution of ferrocene (1 mM) and tetrabutylammonium perchlorate (counterion, 0.1M) in propylene carbonate measured with just two electrodes (insulated tip and Pt counter electrode) and three electrodes (substrate, insulated tip, and Pt counter electrode). In the two-electrode system, the area of the insulated tip is significantly smaller than the area of the Pt counter electrode, so all of the applied potential will drop across the working electrode. This arrangement results in the blue voltammogram shown in Figure 3 with the midpoint of ferrocene oxidation at an applied potential of ∼0.5 V. Repeating the measurement with the three-

dx.doi.org/10.1021/nl404459q | *Nano Lett.* XXXX, XXX, XXX−XXX

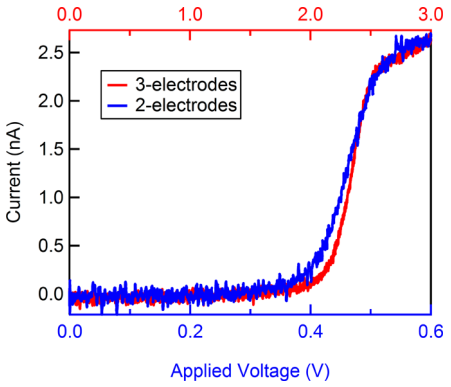

Figure 3. Linear sweep voltammograms of ferrocene (1 mM) in propylene carbonate with tetrabutylammonium perchlorate (0.1 M). In the 2-electrode circuit (blue curve, bottom axis), current is measured through the STM tip while applying the voltage to the Pt gate electrode keeping the substrate floating (unconnected). In the 3-electrode circuit (red curve, upper axis), the same measurement is performed while grounding the substrate, allowing for a current path through the substrate. Both voltammograms are recorded at a sweep rate of 100 mV/s.

electrode arrangement yields the red curve (current is still measured through the tip, while the substrate electrode is grounded and thus provides a current pathway). In this case, because of the extra surface area only a fraction of the applied potential actually drops across the working electrodes (tip and substrate), and the current from the ferrocene oxidation reactions does not peak until an applied potential of ~2.5 V. Although current is passing through both the tip and the substrate, we are still only concerned with measuring the current through the tip. Comparing the onset of current between the two curves, we determine that the applied gate potential needs to be scaled by a factor of 5. Additionally, we have carried out measurements using a geometry where the Pt gate electrode is much larger than the Au tip/substrate (source/drain) electrodes (see discussion in Supporting Information and Figure S4). Indeed, we find that by changing the area ratios, we are able to impact how the gate potential drops across the molecular junction.

We show in Figure 4, the conductance peak positions measured for both molecules against the scaled gate potential (markers) and fit this data to a single-Lorentzian peaked at an energy ϵ from E_F with a full width at half-maximum of Γ, which describes transport for the two molecules (solid lines, including high-G and low-G for molecule **2**). We determine from this fit the coupling Γ of the conducting orbital to the leads, and ϵ, the energy difference between conducting orbital, and E_F without a gate. For molecule **1**, we find that a coupling Γ of 0.12 eV and a resonance position of −2.0 eV relative to E_F. For molecule **2**, we get Γ and ϵ of 0.04 and 1.5 eV for the high-G junctions and 0.02 and 1.4 eV for the low-G junctions. We see that for molecule **2**, the high-G junctions are better coupled (larger Γ) than the low-G junctions in agreement with previous work on 4,4′-bipyridine junctions.[27]

We further compare these fits with transport calculations based on a parameter-free, scattering-states, self-energy corrected density functional theory (DFT+Σ) approach (dashed lines in Figure 4, see Supporting Information for details). We model the junctions with a unit cell of 7 layers of 16 (4 × 4) gold atoms with the molecule bound to a trimer Au tip structure on both sides. Initial geometries for both molecules **1** and **2** are adapted form previous work.[28,29] Relaxed geometries are obtained using DFT with a gradient-corrected exchange-correlation functional (GGA-PBE) using a double-ζ-basis set implemented in the SIESTA package.[30−32] Transmission functions are calculated using a self-energy corrected scattering-states approach DFT+Σ,[33,34] implemented in the SCARLET code[35] as detailed in the Supporting Information. In Figure 4, we overlay the calculated transmission curves for molecule **1** and **2** (high G and low G) and find a good agreement in both the position of the resonance and its width between experiment and theory.

Such transmission functions as described above detail the probability that an electron of a given energy incident upon the molecular junction will be transmitted from one lead to the other through the molecule. In the present case of off-resonant tunneling, such probability is strongly dependent on the relative alignment of the energy of the frontier orbital of the molecule to the Fermi energy of the leads. By applying an electrolyte gate, we are able to modulate this relative alignment, bringing the relevant orbitals closer or further from resonance; this is modifying the barrier for tunneling experienced by the electrons. In our experiments, since a small source-drain bias (25 mV) is applied to the molecular junction, the measured conductance approximately corresponds to transmission at one point along the energy axis. Upon gating the molecular junctions, the transmission function is rigidly shifted with respect to the original E_F.[10,36,37] These experiments therefore

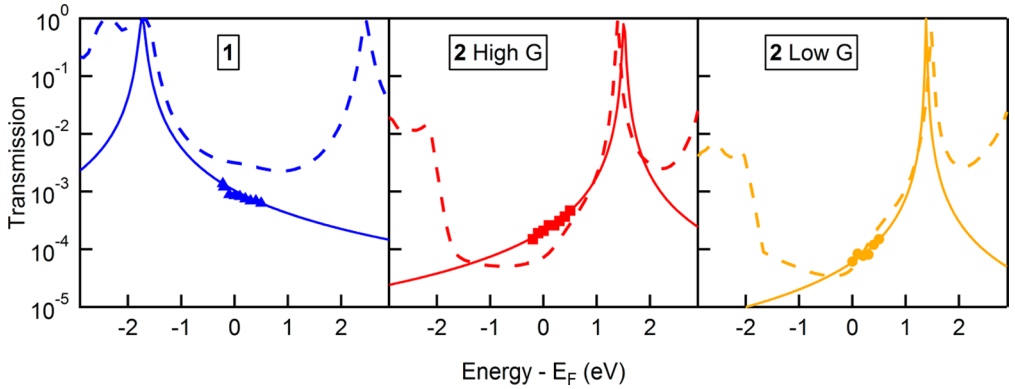

Figure 4. Conductance data for molecules **1** and **2** plotted against the potential drop at the working electrode (markers) fit with a single-Lorentzian transmission model (solid lines). The DFT+Σ calculated transmission functions are overlaid as dashed lines.

dx.doi.org/10.1021/nl404459q | Nano Lett. XXXX, XXX, XXX−XXX

allow a direct mapping of the transmission functions of molecular junctions.

In summary, we have tuned the conductance of electrochemically inactive molecules using an electrolytic gate. Qualitatively, we see that conductance shifts in the expected direction upon application of positive and negative gate potentials for junctions whose transport is dominated by HOMO or LUMO resonances. Furthermore, using quantitative self-energy corrected DFT-based conductance calculations, we have demonstrated that the experimentally obtained conductance values as a function of gate potential trace out the predicted molecular junction transmission functions.

■ ASSOCIATED CONTENT

Ⓢ Supporting Information

Additional experimental data, analysis details, and a description of the density functional theory calculations. This material is available free of charge via the Internet at http://pubs.acs.org.

■ AUTHOR INFORMATION

Corresponding Author

*E-mail: lv2117@columbia.edu.

Notes

The authors declare no competing financial interest.

■ ACKNOWLEDGMENTS

We thank Philip Kim and Giselle Elbaz for fruitful discussions. This work was supported primarily NSF DMR award and by the Alfred P. Sloan Foundation. Portions of this work were performed at the Molecular Foundry and supported by the Division of Materials Sciences and Engineering (Theory FWP) under the auspices of the Office of Basic Energy Sciences of the U.S. Department of Energy under Contract No. DE-AC02-05CH11231. The synthetic part of this work was supported as part of the Center for Re-Defining Photovoltaic Efficiency through Molecular-Scale Control, an Energy Frontier Research Center funded by the U.S. Department of Energy (DOE), Office of Science, Office of Basic Energy Sciences under award number DE-SC0001085.

■ REFERENCES

(1) Aviram, A.; Ratner, M. A. *Chem. Phys. Lett.* **1974**, *29* (2), 277−283.
(2) Xu, B. Q.; Xiao, X. Y.; Tao, N. J. *J. Am. Chem. Soc.* **2003**, *125* (52), 16164−16165.
(3) Venkataraman, L.; Klare, J. E.; Tam, I. W.; Nuckolls, C.; Hybertsen, M. S.; Steigerwald, M. L. *Nano Lett.* **2006**, *6* (3), 458−462.
(4) Mishchenko, A.; Vonlanthen, D.; Meded, V.; Burkle, M.; Li, C.; Pobelov, I. V.; Bagrets, A.; Viljas, J. K.; Pauly, F.; Evers, F.; Mayor, M.; Wandlowski, T. *Nano Lett.* **2010**, *10* (1), 156−163.
(5) Haiss, W.; Wang, C. S.; Grace, I.; Batsanov, A. S.; Schiffrin, D. J.; Higgins, S. J.; Bryce, M. R.; Lambert, C. J.; Nichols, R. J. *Nat. Mater.* **2006**, *5* (12), 995−1002.
(6) Song, H.; Kim, Y.; Jang, Y. H.; Jeong, H.; Reed, M. A.; Lee, T. *Nature* **2009**, *462* (7276), 1039−43.
(7) Park, J.; Pasupathy, A. N.; Goldsmith, J. I.; Chang, C.; Yaish, Y.; Petta, J. R.; Rinkoski, M.; Sethna, J. P.; Abruna, H. D.; McEuen, P. L.; Ralph, D. C. *Nature* **2002**, *417* (6890), 722−725.
(8) Perrin, M. L.; Verzijl, C. J. O.; Martin, C. A.; Shaikh, A. J.; Eelkema, R.; van EschJan, H.; van Ruitenbeek, J. M.; Thijssen, J. M.; van der Zant, H. S. J.; Dulic, D. *Nat. Nanotechnol.* **2013**, *8* (4), 282−287.
(9) Liang, W.; Shores, M. P.; Bockrath, M.; Long, J. R.; Park, H. *Nature* **2002**, *417* (6890), 725−729.
(10) Minot, E. D.; Janssens, A. M.; Heller, I.; Heering, H. A.; Dekker, C.; Lemay, S. G. *Appl. Phys. Lett.* **2007**, *91* (9), 093507−3.
(11) Heller, I.; Chatoor, S.; Männik, J.; Zevenbergen, M. A. G.; Dekker, C.; Lemay, S. G. *J. Am. Chem. Soc.* **2010**, *132* (48), 17149−17156.
(12) Panzer, M. J.; Frisbie, C. D. *Adv. Mater.* **2008**, *20* (16), 3177−3180.
(13) Cho, J. H.; Lee, J.; Xia, Y.; Kim, B.; He, Y.; Renn, M. J.; Lodge, T. P.; Daniel Frisbie, C. *Nat. Mater.* **2008**, *7* (11), 900−906.
(14) Kim, S. H.; Hong, K.; Xie, W.; Lee, K. H.; Zhang, S.; Lodge, T. P.; Frisbie, C. D. *Adv. Mater.* **2013**, *25* (13), 1822−1846.
(15) Misra, R.; McCarthy, M.; Hebard, A. F. *Appl. Phys. Lett.* **2007**, *90* (5), 052905−3.
(16) Kergoat, L.; Herlogsson, L.; Piro, B.; Pham, M. C.; Horowitz, G.; Crispin, X.; Berggren, M. *Proc. Natl. Acad. Sci. U.S.A.* **2012**, *109* (22), 8394−8399.
(17) Ono, S.; Miwa, K.; Seki, S.; Takeya, J. *Appl. Phys. Lett.* **2009**, *94*, 063301.
(18) Díez-Pérez, I.; Li, Z.; Guo, S.; Madden, C.; Huang, H.; Che, Y.; Yang, X.; Zang, L.; Tao, N. *ACS Nano* **2012**, *6* (8), 7044−7052.
(19) Li, X.; Xu, B.; Xiao, X.; Yang, X.; Zang, L.; Tao, N. *Faraday Discuss.* **2006**, *131* (0), 111−120.
(20) He, J.; Fu, Q.; Lindsay, S.; Ciszek, J. W.; Tour, J. M. *J. Am. Chem. Soc.* **2006**, *128* (46), 14828−14835.
(21) Haiss, W.; Albrecht, T.; van Zalinge, H.; Higgins, S. J.; Bethell, D.; Höbenreich, H.; Schiffrin, D. J.; Nichols, R. J.; Kuznetsov, A. M.; Zhang, J.; Chi, Q.; Ulstrup, J. *J. Phys. Chem. B* **2007**, *111* (24), 6703−6712.
(22) Darwish, N.; Díez-Pérez, I.; Da Silva, P.; Tao, N.; Gooding, J. J.; Paddon-Row, M. N. *Angew. Chem., Int. Ed.* **2012**, *51* (13), 3203−3206.
(23) Nagahara, L. A.; Thundat, T.; Lindsay, S. M. *Rev. Sci. Instrum.* **1989**, *60* (10), 3128−3130.
(24) Batra, A.; Darancet, P. T.; Chen, Q.; Meisner, J.; Widawsky, J. R.; Neaton, J. B.; Nuckolls, C.; Venkataraman, L. *Nano Lett.* **2013**, *13* (12), 6233−7.
(25) Kamenetska, M.; Quek, S. Y.; Whalley, A. C.; Steigerwald, M. L.; Choi, H. J.; Louie, S. G.; Nuckolls, C.; Hybertsen, M. S.; Neaton, J. B.; Venkataraman, L. *J. Am. Chem. Soc.* **2010**, *132* (19), 6817−6821.
(26) Fatemi, V.; Kamenetska, M.; Neaton, J. B.; Venkataraman, L. *Nano Lett.* **2011**, *11*, 1988−1992.
(27) Quek, S. Y.; Kamenetska, M.; Steigerwald, M. L.; Choi, H. J.; Louie, S. G.; Hybertsen, M. S.; Neaton, J. B.; Venkataraman, L. *Nat. Nanotechnol.* **2009**, *4* (4), 230−234.
(28) Park, Y. S.; Widawsky, J. R.; Kamenetska, M.; Steigerwald, M. L.; Hybertsen, M. S.; Nuckolls, C.; Venkataraman, L. *J. Am. Chem. Soc.* **2009**, *131* (31), 10820−10821.
(29) Widawsky, J. R.; Darancet, P.; Neaton, J. B.; Venkataraman, L. *Nano Lett.* **2012**, *12* (1), 354−358.
(30) Ordejón, P.; Artacho, E.; Soler, J. M. *Phys. Rev. B* **1996**, *53* (16), R10441−R10444.
(31) José, M. S.; Emilio, A.; Julian, D. G.; Alberto, G.; Javier, J.; Pablo, O.; Daniel, S.-P. *J. Phys.: Condens. Matter* **2002**, *14* (11), 2745.
(32) Perdew, J. P.; Burke, K.; Ernzerhof, M. *Phys. Rev. Lett.* **1996**, *77* (18), 3865−3868.
(33) Quek, S. Y.; Venkataraman, L.; Choi, H. J.; Louie, S. G.; Hybertsen, M. S.; Neaton, J. B. *Nano Lett.* **2007**, *7* (11), 3477−3482.
(34) Quek, S. Y.; Choi, H. J.; Louie, S. G.; Neaton, J. B. *Nano Lett.* **2009**, *9* (11), 3949−3953.
(35) Choi, H. J.; Cohen, M. L.; Louie, S. G. *Phys. Rev. B* **2007**, *76* (15), 155420.
(36) Daghero, D.; Paolucci, F.; Sola, A.; Tortello, M.; Ummarino, G. A.; Agosto, M.; Gonnelli, R. S.; Nair, J. R.; Gerbaldi, C. *Phys. Rev. Lett.* **2012**, *108*, 066807.
(37) Yuan, H.; Shimotani, H.; Ye, J.; Yoon, S.; Aliah, H.; Tsukazaki, A.; Kawasaki, M.; Iwasa, Y. *J. Am. Chem. Soc.* **2010**, *132* (51), 18402−18407.